Failure Analysis of Engine Valve Spring

Yogesh Mahajan, D. V. Moghe, D. R. Peshwe
Department of Metallurgical and Materials Engineering,
Visvesvaraya National Institute of Technology, Nagpur,
Maharashtra, India

***Abstract*— Engine valve springs are subjected to several thousands cycles per minute of repeated stress. These are required to have extremely high reliability over extended period of times. Principal factor that decides spring steel quality depends on size distribution of oxide inclusion. Improvements of fatigue strength have been achieved mainly by increasing the strengths of oil tempered wires; however this approach has a limit at a tensile strength of 1,800 MPa above which the fatigue strength tends to deteriorate due to the fracture at non-metallic inclusions and surface irregularities. This paper presents the classical failure analysis of an Engine valve springs which failed in service. The fractured surfaces as well as the surface of the spring close to the fractured surface were examined in a scanning electron microscope at suitable magnifications. Optical microscopy was performed to evaluate the basic microstructure of the as received material. Detailed electron microscopic studies, EDAX analysis and X-ray mapping have indicated that the failure was due the presence of non metallic, non deformable inclusions near the surface of the spring material.**

***Keywords*—Engine valve spring; Fracture; EDAX analysis; X-ray mapping; inclusion**

I. INTRODUCTION

Engine valve springs permit both intake and exhaust valves to alternately open and close as the engine is in operation. This process occurs for each valve for each engine cycle, and occurs many millions of times over the lifetime of the engine. The spring is subjected to several thousands cycles per minute of repeated stress at elevated temperatures are required to have extremely high reliability over extended period of times. The valve spring on the engine have to guarantee running distance 100,000km.Valve Springs thus need to have higher life and lower loss properties. Engine valve spring steel is high strength steel and is sensitive to inclusion in steel. Accumulated fatigue in the spring break to damage from inclusion. Therefore size and a number of inclusions in spring steel have to reduce from steel making process.

It is important that the composition ratio of alumina in inclusion is controlled in below 20% and the most inclusions are lengthened during the hot rolling process. The thickness size of inclusions is controlled below 10μm and these inclusions are independent of fatigue in the rotary banding test [1].

This spring is designed to sustain the endurance testing for 10 million cycles for tractor engine. Improvements of fatigue strength have been achieved mainly by increasing the strengths of oil-tempered wires; however, this approach has a limit tensile strength of 1800MPa above which the fatigue strength tends to deteriorate due to the fracture at non-metallic inclusions. Fig.1 signifies the effect of tensile strength of steel wire for valve spring on fatigue strength and on initiation site of fracture [2].

Material	Initiation of fracture		Chemical compositions (wt%)				
	Inclusion	Surface	C	Si	Mn	Cr	V
Si-Cr Steel	●	○	0.55	1.40	0.70	0.70	–
Cr-V Steel	▲	△	0.67	0.25	0.75	0.50	0.20
Plain carbon steel	–	□	0.82	0.25	0.45	–	–

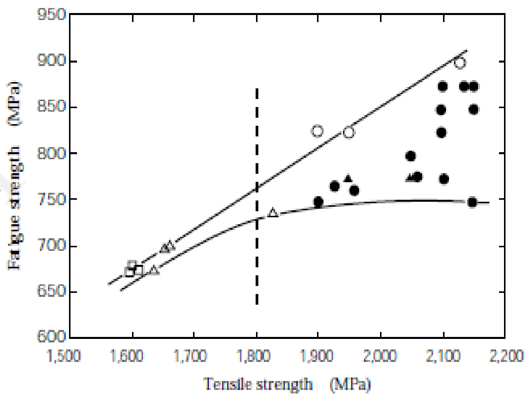

Fig. 1 Effect of tensile strength of steel wire for valve spring on fatigue strength and on initiation site of fracture

Engine valve springs are subjected to several thousands cycles per minute of repeated stress. Assuming no defect in spring wire, the fatigue strength is calculated by the following equation [3].

$$\sigma_w = 1.6HV \text{.........................(1)}$$

With the presence of internal defects such as inclusions larger than 10μm Murakami estimated [3] that the fatigue strength to be,

$$\sigma_w = \frac{1.56(HV + 120)}{\sqrt{area^{1/6}}}\left(\frac{(1-R)}{2}\right)^{a}$$

$$where, R = \frac{(\sigma_m - \sigma_w)}{(\sigma m + \sigma w)}$$

$$\alpha = 0.226 + HV * 10^{-4}$$

$$area = defect \quad area,$$

$$\sigma_m = average \quad stress$$

The formula indicates that an increase in hardness and reduction in defect-size are required to improve fatigue strength.

Non metallic size should be less than the 10 µm size. Non metallic inclusion should be of low melting, soft, glassy and should have form factor >>3 in the hot worked/cold drawn state. Softer inclusions are crush easily during the hot rolling process without decohesion at the inclusion-matrix interface. The presence of MgO in the inclusion is extremely detrimental for fatigue strength and hence to be maintained to lower level. The need to prevent Mg/MgO joining the melt is crucial.

Beside inclusion rating other factors which affect the performance of spring are thermal treatments, surfaced modifications, etc. Using steel grade with High Si(1.80-2.20%)-Cr(0.85-1.05%)-V(0.05-0.15%) steel with nitriding reduces the probability of failure and increase the life of the spring. It can also reduce the weight of the spring and thereby improving fuel consumption which reduces CO_2 emission. Increasing stress reliving time helps in reducing the stress level and subsequent failure. Reducing surface irregularities decreases the chances of failures. The modifications of the spring process technologies, including improved shot-peening and application of new surface treatments (nitriding), will be needed for the further improvements. Nitriding to the present steel grade improves the fatigue strength by a factor of approximately 1.3[3]. Proper care should be taken during fitment and alignment of the spring.

II. FAILURE HISTORY

The customer returned the fractured engine valve spring sample after a premature failure in service after 61 hours in field. The springs are originally produced from cold drawn, oil hardened and tempered SWOSC-B steel wire [Si-Cr steel]. Spring from 4.50 mm diameter wire is manufactured by coiling, stress reliving at 400 ^{0}C for 30 min, end grinding, shot peening, and again stress reliving at 250 ^{0}C for 30 mins. Tensile strength specified is about 1,810-1,960 MPa with 45% min reduction in area.

The failed engine valve spring material is demonstrated in fig. 2. The detailed metallurgical investigations were carried out on the fractured spring sample which included visual examination, optical microscopy, scanning electron microscopy and X-ray mapping.

Fig.2 Broken Engine valve spring

III. EXPERIMENTAL PROCEDURE

A. *Visual Examination*

Visual examination of the spring sample revealed a generally smooth surface without any apparent indication of cracks at the outer surface. Engine valve spring, end ground at both the ends fractured at two locations - 3rd coil from top and bottom. However, the fractured portion of the sample revealed a brighter shiny surface typical of brittle fracture and is shown in fig. 3. It shows a chevron pattern radiating away from the origin of the crack as indicated in Fig. 4. The other end of the spring sample also revealed the fine grained fracture as demonstrated in Fig. 5.

Fig.3 SEM photograph of fractured surface. Selected area is magnified in SEM image no.4

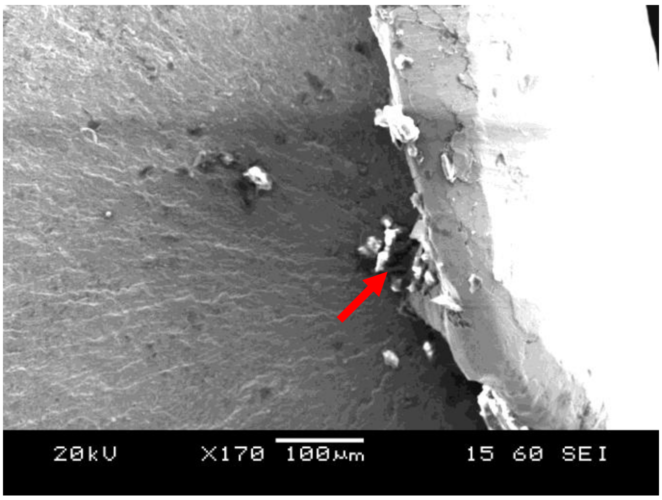

Fig.4 Magnified view of SEM image fig.4 indicating chevron pattern and origin of the crack

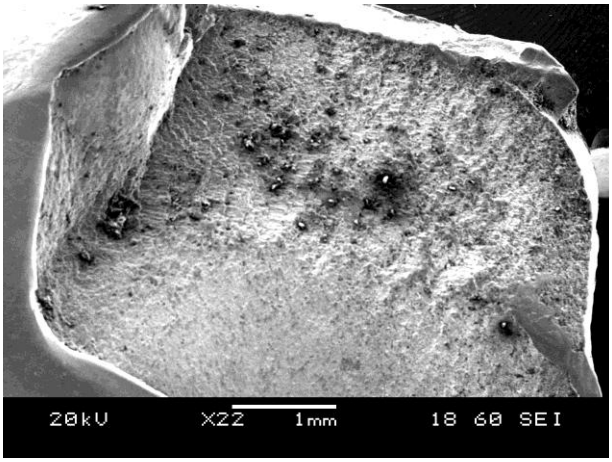

Fig.5 SEM photograph of fractured surface of other end of the spring sample

B. Chemical Analysis

The chemical analysis indicates that the spring Material confirms to the specification - JIS 3568 G SWOSC-B steel which is a Cr- Si steel grade.

Table 1--Result of chemical analysis.

Element	%C	%Mn	%Si	%Cr	%S	%P
Specified	0.51-0.59	0.50-0.90	1.20-1.60	0.50-0.80	0.035 max	0.035 max
Actual	0.53	0.78	1.45	0.72	0.015	0.015

C. Micro Hardness test

Hardness specified for the engine valve spring is in the range of 520-560 Hv 0.3 Kg while actual hardness observed on the surface is in the range of 534 to 545 Hv and for the core 542-555 Hv 0.3 Kg which meets the manufacture's specification. These data suggest that spring failure is not associated with violation of heat treatment technology.

D. Optical Microscopy

For metallographic inspection, spring samples are mounted in longitudinal as well as in transverse direction and analyzed. The optical microscopy of the spring sample revealed a normal hardened and tempered structure typical of high strength spring steel, as shown in fig.6. It shows tempered martensite in the structure.

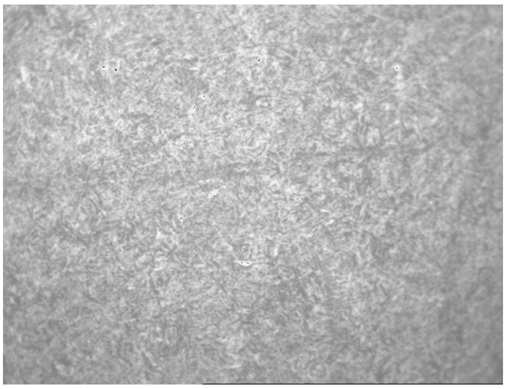

Fig.6 Optical microstructure at 500X of the sample revealing tempered martensite

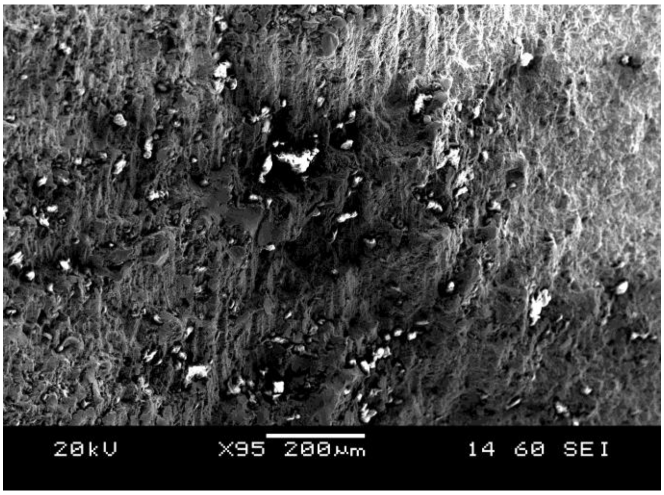

Fig.7 SEM photograph of fractured surface

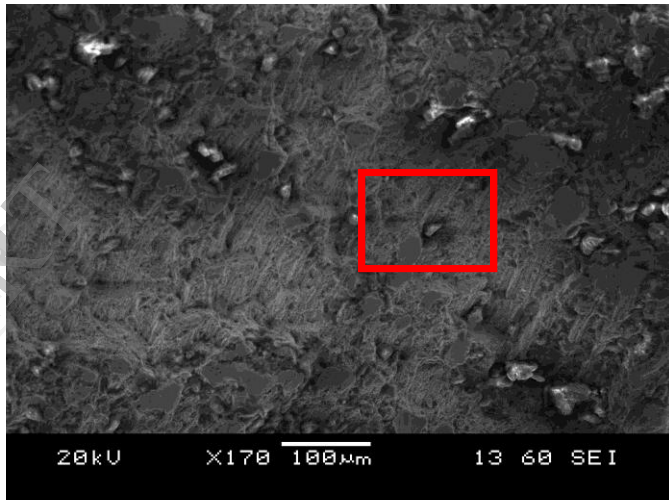

Fig.8 SEM photograph of fractured surface

E. Scanning electron microscopy

The scanning electron microscopy was performed using a JEOL SEM model JSM 6380A with an energy dispersive system. It is equipped with a light element detector and software for quantitative chemical analysis.

Different fractured surfaces are shown in fig.7 and fig.8. Examination of the fractured surface exhibited the familiar fibrous fracture typical of a high strength spring material as shown in fig.7. It can also be deduced that the material is a fine-grained component. At some locations, fractured surface as indicated in fig. 8 exhibits a combination fractured mode of ductile and brittle fracture. Fractured surface shows the dimple fracture surface characteristic of the ductile metal as well as cleavage fracture surface characteristic of the brittle metal.

Similarly, other SEM photographs are also analyzed and shown in the figures 9a, 10a, 11a, 11b and 12a. It shows elongated dimples at the shear lips. . SEM images of fractured surface shows inclusion matrix interface decohesion. The size of the non metallic particle observed is about 10-20 µm.

F. Energy dispersion system

The red marked region in the Fig.8 is magnified to 3000X and shown in Fig. 9a. After analyzing, the size of the entrapped particle observed is about 10 - 20 µm size. The white regions in the fractured surface are the distinguished non metallic inclusion particles in the matrix. The EDAX analysis of the entrapped inclusion shows the presence of major constituent elements such as Silicon (25 at%), Aluminium, Magnesium and Oxygen. The adjacent portion of the entrapped particle was also analyzed by elemental image analysis. It shows intense peak of iron and small peaks for the Silicon (1.5at%), Aluminium and Oxygen. This can be seen from the EDAX graph Fig. 9b-9c.

Similarly, other SEM photographs are also analyzed and shown in the figure 9 and 10 with EDAX analysis. It shows elongated dimples at the shear lips. SEM images as indicated in fig.9a, 10a, 11a and 11b of fractured surface shows inclusion matrix interface decohesion. The intensity of silicon, Aluminium, Magnesium and Oxygen peak is more on the entrapped particle than the adjacent area. SEM images of fractured surface as in fig.11a shows inclusion protruding out from the matrix. The selected area is magnified at 3700X. It clearly shows the matrix interface decohesion as indicated in fig.11b. The intensity of silicon, Aluminium and oxygen peak is more on the entrapped particle than the adjacent area. This shows the presence of Silicon, Aluminium, Calcium Oxygen, and Magnesium as major constituents in the inclusion.

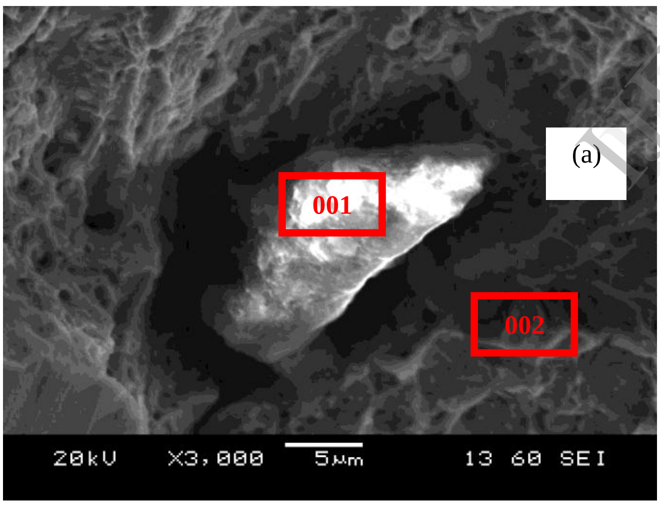

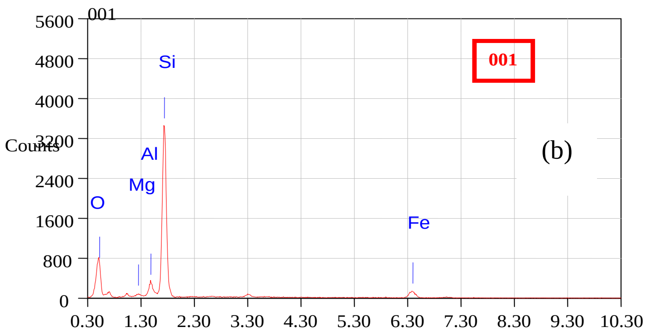

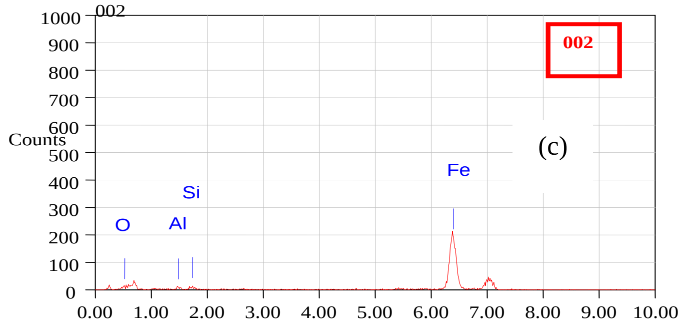

Fig.9 Magnified view of the region shown in fig.7 indicating non metallic inclusion (a) with the EDAX spectrum taken from the inclusion region (b) and near by region (c)

The ZAF Method Standardless Quantitative Analysis indicates the presence of Silicon is about 15-25at%, Oxygen about 35-40at% and Magnesium about 15at% at the non metallic inclusion area while in the rest portion, Silicon is about 1.5 at% and Oxygen about 5 at%. The size of the non metallic particle observed is about 10-20 µm.

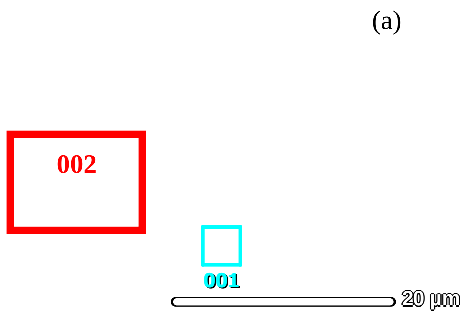

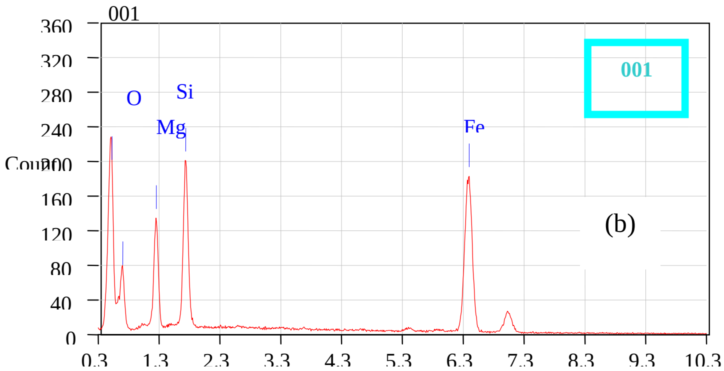

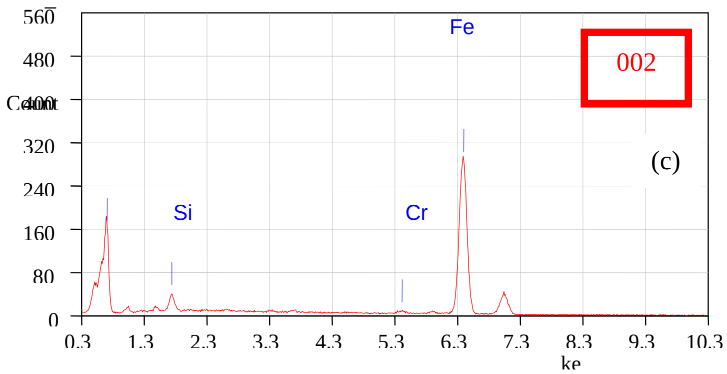

Fig.10 SEM photograph at 2200X of the fractured surface indicating non metallic inclusion (a) with the EDAX spectrum taken from the inclusion region (b) and adjacent area (c).

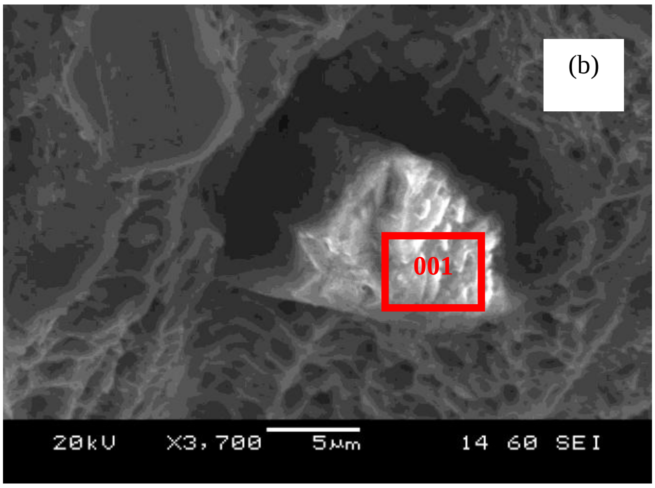

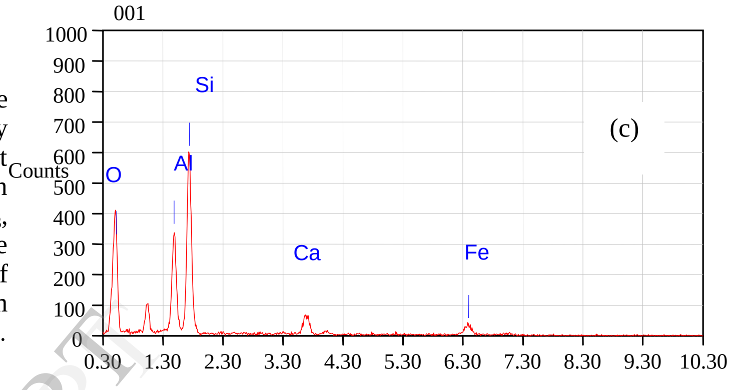

G. *Energy dispersion system*

In addition to examining the fracture and the surface of the material, the inclusions were examined by Elemental X-ray Image analysis. It gives colour pixels equal to the element concentration. The location of silicon, aluminium and oxygen elements are shown in the Fig. 12. Inclusions of SiO_2, Al_2O_3, MgO-Al_2O_3 are known to cause breakage of valve springs. The analysis suggests that these are the non-metallic particles of oxides of Silicon (i.e SiO_2) , Aluminium (i.e Al_2O_3), Calcium (CaO) and Magnesium (MgO) with the size of about 10-20 µm.

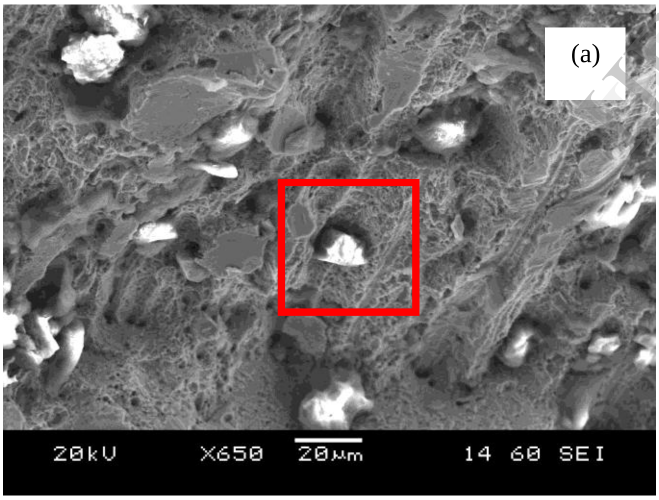

Fig.11 SEM photograph of the fractured surface indicating non metallic inclusion at 650X (a), Magnified view of the non metallic inclusion at 3700X (b) with the EDAX spectrum taken from the inclusion region (c)

From the above observations we can conclude that the presence of hard, non deformable, 10-20 µm size inclusions are the potential sites for the crack initiation and subsequent failure.

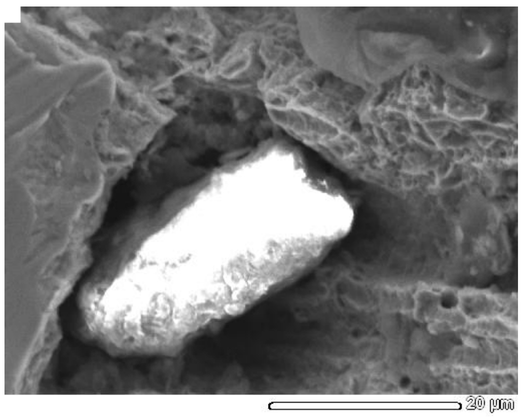

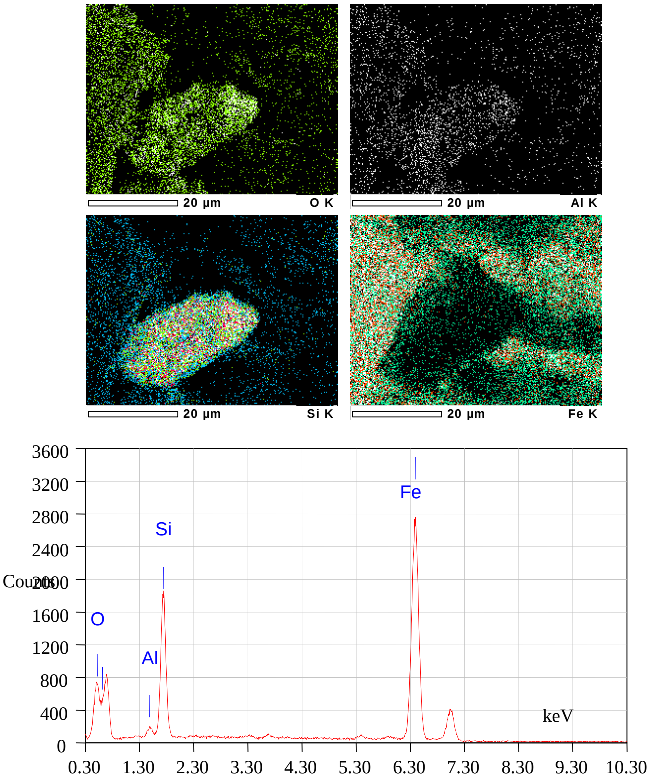

Fig.12 SEM photograph at 2300X with the X-ray Mapping and EDAX analysis

IV. CONCLUSION

It is a shear type of failure originated from the sub surface region. Either during hot working and /or during cold drawing of wires, the matrix has deformed more than the non metallic inclusions. Thus inclusion matrix interface decohesion takes place leading to formation of microcracks in the matrix. These cracks would grow when the spring is put into service and cause premature failure.

[1] Y. T. Shin, J. D. Seo, S. W. Choi and J. S. Lee, Rapid inclusion determination method for spring steel, *Posco Technical Report* 2007, VOL. 10 -01

[2]] N. Ibaraki, R&D Kobe Steel Engineering Reports, 2000 ,p.27,Vol.50-3

[3] Y. Murakami, *Effects of Small Defects and Nonmetallic Inclusions*, Yokendo Ltd,1993, p.90